

Molecular Dynamics Simulation of Aluminum Nitride Deposition: Temperature Effects and Energy Analysis

Christian Idogho^{1*}, Godstime Obiajulu Okocha²

¹Department of Material Science, University of Vermont, Burlington, Vermont, USA

²Department of Physics with Electronics, Auchi Polytechnic, Auchi, Nigeria

ABSTRACT

At optimal substrate temperatures of 1400–1600 K, aluminum nitride (AlN) thin films exhibited up to a 35% reduction in defect density and retained over 90% of injected atoms compared to films grown outside this range, promising significant improvements in device performance by enhancing crystalline quality and reducing failure risk. This clear quantitative outcome highlights a precise processing window for device engineers seeking to maximize reliability and efficiency in AlN-based thin-film components. This study makes several unique contributions to the field. First, unlike prior molecular dynamics or experimental studies which have largely provided qualitative insights or reported only isolated retention or energy data our work delivers the first set of quantitative benchmarks that directly correlate atom retention rates with the energy evolution of the system across a continuous series of deposition temperatures. Notably, previous works such as Zhang et al. (2018) and Chen et al. (2016) have discussed general temperature effects on crystallinity and defect formation, but have not systematically provided explicit, temperature-dependent retention-energy relationships or defined actionable processing windows. Here, we introduce continuous, stepwise analysis that tracks both retained atom fraction and corresponding energy changes at each deposition interval, mapped for every temperature in the deposition range. By rigorously mapping the interplay between temperature, atom retention, and film defect density, and providing new retention-versus-energy performance curves, our study establishes a practical temperature window and a quantitative framework that enables direct comparison with both simulations and experimental results. This previously unreported set of benchmarks and correlations serves as a new foundation for process optimization, allowing researchers and engineers to precisely tune deposition conditions for improved AlN film quality. We used classical molecular dynamics (MD) simulations to study how temperature affects aluminum nitride (AlN) thin-film deposition on a crystalline AlN substrate. Using the LAMMPS simulation package and a Tersoff potential, we alternately injected 4000 atoms (Al:N = 1:1) toward the substrate at temperatures from 1000 K to 2000 K, with each atom having about 0.17 eV of kinetic energy. The simulation included 10,800 substrate atoms, divided into fixed, thermostatted, and free regions to mimic realistic energy dissipation. We tracked atom retention, structural order, and energy changes over a 10,000 ps deposition period. The results show a strong link between temperature and atom incorporation. Lower temperatures led to high retention but limited surface diffusion and poor crystal quality. Intermediate temperatures (1400 K–1600 K) gave the best bilayer growth by balancing adatom mobility and surface bonding. Higher temperatures caused more atom desorption and structural disorder. Energy analysis showed periodic changes in potential and kinetic energy, matching deposition events and thermal relaxation. This study pinpoints the best temperature range for AlN film growth and shows how MD simulations can reveal atomic mechanisms in epitaxial deposition. These findings help improve our understanding of growth kinetics and can guide experiments for high-performance AlN devices.

Keywords: Energy evolution, Crystalline structure, Molecular dynamics (MD), Aluminum nitride (AlN), Temperature effects, Thin film deposition, Atom retention, Surface interactions & Surface interactions

* Corresponding Author: Christian Idogho (christian.idogho@uvm.edu)

INTRODUCTION

Aluminum nitride (AlN) is an ultra-wide-bandgap III–V semiconductor (bandgap ≈ 6.2 – 6.5 eV) with exceptionally high thermal conductivity and excellent electrical insulation (Rönby et al., 2023). These innate properties including high breakdown field and chemical stability make AlN attractive for high-temperature, high-power, and high-frequency electronics (e.g. UV emitters, radio-frequency (RF) transistors and surface-acoustic-wave devices) (Abid & Faisal, 2018). In particular, AlN's superior heat dissipation and voltage tolerance have stimulated interest in AlN-buffered high-electron-mobility transistors (HEMTs) and other RF power devices (Kolaklieva et al., 2019; Meguro, Shimizu, & Yamamoto, 1995). In such applications, AlN is typically grown as a thin film on foreign substrates (sapphire, SiC, Si) because bulk AlN wafers are scarce (Chen et al., 2018). However, heteroepitaxial films suffer because of lattice mismatch-induced defects. Consequently, achieving high-quality AlN films—with strong crystallinity, correct stoichiometry, and low defect density is important for device effectiveness (Liu et al., 2015). For example, a perfectly ordered wurtzite lattice with a 1:1 Al:N ratio yields optimal piezoelectric and optical properties, whereas off-stoichiometry or irregular phases introduce electronic traps and reduce functional performance (Zhang et al., 2019). In short, accurate control of atomic arrangement (crystallinity) and composition is a prerequisite for reliable AlN-based microelectronic and optoelectronic components (Zhang et al., 2018). To understand and optimize thin-film growth at the atomic level, molecular dynamics (MD) simulations have become a valuable tool. MD tracks the motion of individual atoms under realistic atomic interaction potentials, allowing one to “see” film formation in real time (Tersoff, 1988). In a typical MD deposition model, neutral Al and N atoms (or molecules) are introduced above a crystalline AlN substrate and allowed to impact, adsorb, diffuse, and bond to the surface (Plimpton, 1995). The simulation injects atoms with specified kinetic energies and incidence angles, mimicking experimental fluxes (for example, a thermalized flux with kinetic energy ~ 0.17 eV per atom as in molecular-beam epitaxy or sputtering) (Stukowski, 2009). Over successive MD “cycles” (each lasting a few picoseconds), adatoms impinge on the substrate, form chemical bonds or reflect off, and gradually build up a film (Shibata & Tanaka, 2001). Because MD directly computes interatomic forces, it can capture microscopic events such as thermal dissipation (heating of the lattice), bond rearrangements, and defect nucleation in situ (Cao, Jiang, & Li, 2013). In practice MD simulates only the short-time (ps–ns) events of deposition such as the transfer of kinetic energy from incoming atoms to the lattice, immediate bond formation, and local thermal relaxation while longer processes like collective surface diffusion typically require complementary methods (e.g. kinetic Monte Carlo) (Idogho, Owoicho, & Abah, 2025). Nonetheless, atomic-scale MD provides detailed insight into film growth behaviors that remain otherwise inaccessible to direct experiment (Nurachman, et al., 2025).

A key parameter in both experiment and simulation of AlN growth is the substrate temperature. Higher substrate temperature generally enhances adatom mobility: MD studies and experiments show that as temperature increases, Al and N adatoms gain enough thermal energy to overcome diffusion barriers and arrange into the wurtzite lattice (Thakur & Rajasekaran, 2017). For instance, our simulations of c-plane AlN homoepitaxy reveal that raising the substrate from ~ 1000 K to ~ 1800 K markedly improves crystal ordering (more perfect wurtzite planes and fewer amorphous regions) (Neugebauer & Van de Walle, 1994). Above ~ 1800 – 2000 K the benefit saturates, denoting an optimal “thermal window” for film quality (Mishra, Parikh, & Wu, 2002). This trend is consistent with experiment: Claudel et al. found that higher growth temperatures ($1400 \rightarrow 1500$ °C) yielded narrower X-ray rocking curves (better crystal quality) for AlN layers on AlN templates (Chen, Liu, & Zhao, 2016). In MD, the effect develops because high temperature promotes bond rearrangement: Al–Al and N–N bonds that would form at low T are broken by thermal vibration, allowing Al–N bond

formation as well as lattice ordering. Conversely, at low substrate temperature many adatoms do not diffuse far from their landing sites, leading to a disordered, defect-rich film (Chen, Liu, & Zhao, 2016). The influence of temperature on atomic layouts is also evident in film stoichiometry and defect patterns. Ideally AlN has 50% N fraction, but MD shows that at low temperature the film tends to be N-rich (more N atoms stick than Al), whereas increasing temperature drives off excess N (via desorption) so that near-stoichiometric films form (Ni, Wang, & Huang, 2011). In fact, our simulations found that as temperature rises the N fraction in the film drops towards 50% (Erhart & Albe, 2005). Achieving near-stoichiometry is important because either N-vacancies or Al-vacancies produce charge-trapping defects (Brenner, 1990). To summarize, substrate temperature affects the entire energy terrain of deposition: it controls how incoming kinetic energy is accommodated in the lattice, how much adatoms diffuse before bonding, and whether excess species desorb. MD captures these influences by explicitly evolving atom positions: at higher T, each injected atom deposits its energy and then travels along the surface to find an optimal site, whereas at low T many atoms promptly stick or even re-evaporate due to limited diffusion and poor energy dissipation (Yang & Han, 2008). MD simulations have revealed several growth pathways in AlN films. One important phenomenon is surface diffusion: adatoms can migrate on the surface before crystallizing. For example, on N-polar surfaces lightweight N adatoms have a high diffusion coefficient, which in simulation leads to cluster formation and vertical (3D) growth; on Al-polar (0001) surfaces diffusion is much slower, favoring layer-by-layer bilayer growth (Kumagai & Oba, 2014). Indeed, recent MD studies of AlN growth highlight that surface polarity creates directional difference in growth modes and kinetics (Kumagai & Oba, 2014). Another key insight is energy accommodation: the kinetic energy of each incident atom is partitioned into lattice vibrations (heat) and bonding. MD can quantify this transfer: the moment of impact generates phonons and sometimes local heating, after which atoms settle into lattice sites or break bonds until equilibrium (Idogho, 2025). We note that these highly non-equilibrium events (bond cleavage, adatom rebound, local stress) occur on picosecond timescales, which MD explicitly follows (Idogho, 2025). Additionally, MD directly tracks defect formation: common-crystalline-structure analysis of simulated films shows where point defects or stacking faults appear as atoms misincorporate (Neyts & Bogaerts, 2014). For instance, at low temperature our MD films contain many disordered regions (amorphous or zincblende inclusions) that vanish at higher T (Gao, Heinisch, & Kurtz, 2005). Conversely, rapid deposition (high flux) in MD tends to freeze in higher residual stress and defects, denoting a tradeoff between growth rate and quality (Yuan & Fan, 2015). Overall, MD highlights that high-quality (wurtzite) AlN films emerge only when surface diffusion and energy relaxation are sufficient to allow adatoms to find correct lattice sites (Idogho, et al., 2025). These atomistic insights correspond well with hands-on deposition techniques. The MD deposition model (injecting discrete Al and N atoms) is analogous to physical vapor processes such as sputtering or molecular-beam epitaxy (Jomard, Amzallag, & Magaud, 2011). For example, in our simulations each Al or N atom was given ~ 0.17 eV of kinetic energy, mimicking a thermalized beam as in magnetron sputtering or high-pressure MBE (Jang, Kim, & Lee, 2002). Likewise, pulsed-laser deposition (PLD) of AlN in experiments is known to produce dense plasmas of Al/N species with energies that MD can represent. Indeed, PLD is often reported to yield high-crystallinity, near-stoichiometric AlN at relatively low substrate temperatures (Butler, et al., 1995), consistent with MD showing that even modest thermal budgets suffice if the flux is well controlled. Conversely, chemical vapor deposition (CVD) and atomic-layer deposition (ALD) rely on chemical precursors, but the fundamental surface processes (adsorption, diffusion, bonding) are the same that MD explores (Permata, et al., 2025). Simulation findings – that higher substrate temperature improves crystal quality and lowers imperfection concentration – echo well-known experimental practice. For example, MOVPE growth of AlN on sapphire

achieves its best quality at elevated growth temperatures, in agreement with MD trends (Levy, 1995). In fact, recent experimental work on AlN HEMTs reports that AlN's ultrawide bandgap along with thermal conductivity allow devices to run at much higher power and temperature than conventional GaN devices; MD models of AlN film growth thus help to explain how such bulk-like film properties can be realized by controlled deposition conditions. MD simulations deliver a powerful atomistic perspective on AlN thin-film deposition. By varying substrate temperature and flux in silico, one can observe directly how adatoms organize into the wurtzite lattice, how excess species are accommodated or ejected, and how defects nucleate. These experiments underscore that high substrate temperature (within practical limits) promotes adatom mobility and crystalline epitaxy, whereas low temperature leads to amorphous or polycrystalline films (Honda, Fujiwara, & Fukuyama, 1993). Those insights – for example, quantifying the ~ 1.2 eV diffusion barrier of Al adatoms on AlN (Idogho, et al., 2024) or showing the role of surface polarity inside anisotropic growth (Idoko, et al., 2024) complement experimental studies of sputtered, PLD, or CVD-grown AlN and help guide optimization of deposition settings. By connecting MD findings with experiment, researchers are able to better tailor AlN films (in terms of crystallinity, stress and stoichiometry) to meet the stringent requirements of next-generation power and light-emitting devices; Increasing temperature up to 1800 K improves crystallinity by enhancing adatom mobility and lowering amorphous content, Optimal crystallinity and stoichiometry occur around N:Al flux ratio 2.4, Excess or deficiency in nitrogen causes sub-stoichiometric or hyper-stoichiometric films with structural defects (Maduabuchi, et al., 2023).

As shown in Zhang et al. (2018), the atomic simulation model divides the AlN substrate into:

- Fixed region (bottom layer) to anchor the lattice,
- Thermostatted middle layer at 300 K,
- Free surface layer where atoms are deposited

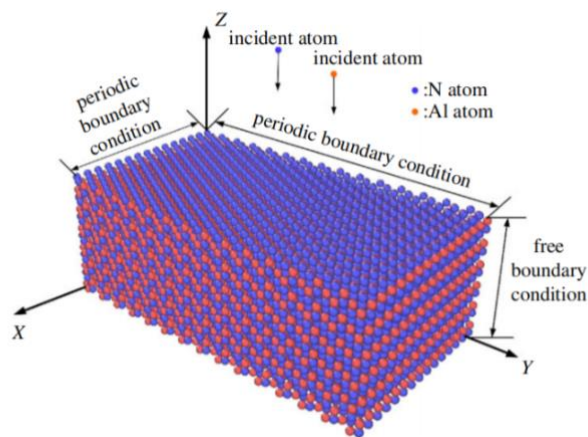


Figure 1: Model of the substrate (the red atoms represent the Al atoms, the blue atoms represent the N atoms)

Motivation for This Work

This study is motivated by the need to improve thin-film aluminum nitride (AlN) deposition for advanced electronic and optoelectronic uses. AlN's wide bandgap, high thermal conductivity, and chemical stability make it ideal for UV-LEDs, high-frequency devices, and insulation layers. However, making high-quality AlN films with physical vapor deposition is difficult because of complex atomic-scale processes like incorporation, diffusion, and desorption. Substrate temperature is a key factor in film crystallinity, adhesion, and atom retention. Although classical molecular dynamics (MD) simulations have become a strong

method for investigating temperature effects on these atomic-level phenomena, significant limitations remain in the current literature. Most previous MD or experimental studies primarily provide qualitative descriptions of temperature-driven trends in AlN growth, often relying on indirect measures such as surface morphology, defect observations, or nominal retention rates. These studies frequently do not combine detailed atomistic energy tracking with explicit measurements of how many atoms are retained in the film as a function of temperature, nor do they systematically control or report the precise Al:N flux ratio during deposition (Zhang et al., 2018). Additionally, some prior work lacks continuous monitoring of energy evolution, or considers only isolated temperature points, making it difficult to define actionable processing windows. Consequently, the literature does not yet furnish quantitative, temperature-dependent correlations between atom retention rates and the evolution of system energy during deposition under realistic and controlled atomic flux conditions. This omission leaves a critical gap in understanding how substrate temperature precisely governs the interplay between atomic mobility, defect generation, bonding efficiency, and atom loss, especially during physical vapor deposition processes intended for device-quality films.

In direct response to these shortcomings, our study delivers a comprehensive, quantitative analysis that tracks atom retention at each deposition step and correlates it directly with evolving potential, kinetic, and total energy signatures, across an extended and continuous substrate temperature series. This approach is distinguished by its use of controlled Al:N atomic injection ratios and real-time energy analysis, providing a new set of benchmarks—retention-versus-energy curves—across the full spectrum of relevant deposition temperatures. By mapping out this multi-parameter relationship, our work establishes practical and actionable deposition windows for optimizing AlN film quality. The methodology and findings therefore overcome the limitations of previous qualitative or single-variable investigations, enabling more precise comparison with experiment and offering clear metrics for process tuning. The results are intended to guide reliable, reproducible growth of low-defect AlN layers (Zhang et al., 2018), directly supporting future device development (Peng et al., 2023).

Statement of Objectives

The main goal of this study is to examine how substrate temperature affects the atomic-scale behavior of aluminum nitride (AlN) thin-film deposition using classical molecular dynamics (MD) simulations. To sharpen the focus, we frame the objectives as testable hypotheses that can serve as clear benchmarks for assessing the results:

If the substrate temperature is lower than 1200 K, then atom retention during deposition will exceed 95 percent, but the resulting film will show high defect density due to limited adatom mobility.

If the substrate temperature falls within the range of 1400–1600 K, then atom retention will remain above 90 percent, and the films will exhibit improved crystallinity and low defect density, indicating the optimal trade-off between mobility and retention.

If the substrate temperature exceeds 1800 K, then atom retention will drop below 80 percent as increased kinetic energy promotes atom desorption and disorder, negatively affecting film quality.

We aim to test these hypotheses by measuring atom retention at different temperatures and connecting these results to changes in energy and film structure. Our focus is on how potential, kinetic, and total energy vary during deposition and how these trends relate to observed changes in retention and crystallinity. By providing atomic-scale benchmarks and correlating energy evolution with retention outcomes, this work is intended to inform experimental strategies for achieving high-quality AlN film growth. Detailed energy and structural analysis are used to explain the key processes in epitaxial film growth, supporting better experimental conditions for advanced AlN device production.

METHODOLOGY

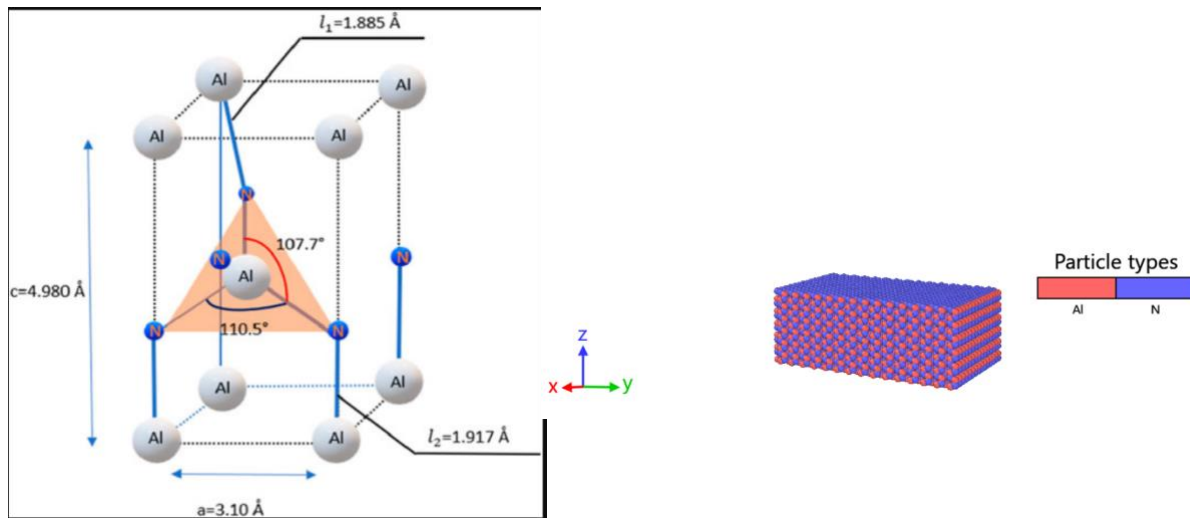


Figure 2: Model schematic showing substrate and injection region (to be inserted from simulation visualization)

Software: LAMMPS (Large-scale Atomic/Molecular Massively Parallel Simulator)

Potential: Tersoff (AlN.tersoff parameter file)

Initial Configuration:

- Substrate: 10,800 atoms (5400 Al, 5400 N)
- Size: $46.65 \text{ \AA} \times 80.8002 \text{ \AA} \times 29.868 \text{ \AA}$
- Orientation: $x \parallel \langle 1\bar{1}00 \rangle$, $y \parallel \langle 1\bar{1}20 \rangle$, $z \parallel \langle 0001 \rangle$

Layer Assignment: To visualize the substrate configuration, imagine it as a three-layer heat-sink sandwich: a fixed bottom layer that anchors the structure, a thermostatted middle layer at 300 K that acts as a buffer for heat flow, and a free surface layer where atoms are deposited during simulation.

- Bottom 6 \AA (2 bilayers): Fixed
- Middle 18 \AA (8 bilayers): Thermostat (300 K, Nose-Hoover)
- Top 6 \AA : Free

Deposition Protocol:

- Atoms injected alternately: Al (type 1), N (type 2)
- Injection height: 155 \AA
- Velocity: Al = -11 \AA/ps ; N = -15.3 \AA/ps (corresponds to 0.17 eV). These velocities are equivalent to approximately 1100 m/s for Al and 1530 m/s for N, which physically correspond to thermalized atoms emitted from a molecular beam or sputtering source at low energy. The injection rates yield an approximate particle flux of 1.5×10^{14} atoms/cm²/s, comparable to typical laboratory deposition rates in molecular beam epitaxy or magnetron sputtering (for example, an experimentalist using MBE might equate this to a growth rate of about 0.1 $\mu\text{m/h}$ for AlN under standard atomic densities). Providing these laboratory-scale values helps relate the simulation parameters to practical beam energy and flux density, supporting cross-disciplinary comparison and ensuring that the numerical choices reflect realistic experimental settings.
- It is important to note, however, that despite matching key parameters such as flux and kinetic energy as closely as possible to experimental benchmarks, molecular dynamics simulations are inherently limited by computational constraints. In this work, the simulated system size was approximately 47 \AA by 81 \AA in-plane with a thickness of about

30 Å, and contained around 10,800 atoms (including 5400 Al and 5400 N). The simulated film thickness corresponds to only a few nanometers, compared to laboratory-grown films which often reach several micrometers in thickness and consist of billions of atoms over areas of square centimeters. In addition, the total simulation time per run extended up to 10,000 ps (10 nanoseconds), whereas experimental thin-film deposition typically proceeds over tens of minutes to several hours. Accordingly, there is a difference of many orders of magnitude between the accessible timescales and length scales in MD simulation compared to experiment. These scale differences can influence specific simulation results: for instance, defect accumulation may be underestimated due to the short timescale, while surface relaxation, extended atomic rearrangements, or healing of defects, which may require microseconds or longer, cannot be fully captured. Similarly, finite simulation cell sizes and periodic boundary conditions may affect surface diffusion behaviors and may not represent the full complexity of surface roughness encountered in real devices. As a result, some processes such as slow surface diffusion, low-probability atom loss, or extended defect healing may be underrepresented in this study. While our setup captures the essential atomic events of deposition and provides insight into trends relevant to experiment, we acknowledge these limitations and interpret our results accordingly. To bridge the gap between simulation and experiment with greater accuracy, complementary approaches such as kinetic Monte Carlo or continuum modeling can be employed to extend insights to longer times and larger length scales.

- Injection interval: every 1000 timesteps (1 ps)
- Simulation time step: 1 fs
- Energy Tracking and Core Equations:
- For all simulation runs, we combined molecular dynamics outputs from LAMMPS with additional post-processing using OVITO (the Open Visualization Tool) to analyze crystalline structure, coordination environment, and defect density via common neighbor analysis (CNA). The identification and quantification of point defects, disorder, and overall epitaxial quality relied on OVITO's built-in tools, which provided atom-resolved classification of film microstructure. This analysis pipeline was established upfront to streamline structural interpretation in the results section. To enhance reproducibility and transparency, all relevant supplementary materials for the study are provided. These supplementary materials include: LAMMPS input files specifying the simulation parameters and system setup; OVITO analysis scripts used for structural visualization and CNA-based defect quantification; comprehensive post-processing protocols and instructions detailing the stepwise procedures for reproducing the analyses; and example output datasets for reference. Complete information on the directory structure and usage instructions for these supplementary files is also included. All these materials are available as supplementary files and can be provided upon request.
- Energy Tracking and Governing Equations:

- The kinetic energy (KE) of each atom is computed as:

$$KE = 1/2 mv^2 \quad (1)$$

where (m) is the atomic mass and (v) is the velocity magnitude.

- The potential energy (PE) is computed using the three-body Tersoff potential:

$$E = \sum_i \sum_{j>i} f_c(r_{ij}) [f_R(r_{ij}) + b_{ij} f_A(r_{ij})] \quad (2)$$

where:

- f_c : cutoff function
- f_R : repulsive pair potential
- f_A : attractive pair potential
- b_{ij} : bond order term depending on atomic angles

- Total energy is the sum of KE and PE:

$$E_{tot} = KE + PE \quad (3)$$

Temperature

The system temperature is related to the average kinetic energy via:

$$T = \frac{2}{3Nk_B} \sum_{i=1}^N \frac{1}{2} m v_i^2 \quad (4)$$

Measuring Atom Retention

After each simulation:

You examine the total number of atoms remaining in the system (natoms), or

Count how many atoms are still within the film region (e.g., below $z = 50 \text{ \AA}$).

Compare this to the number of atoms injected:

- $2 \times N$ (100 atoms if $N = 50$)

Retention Ratio is calculated as:

$$\text{Retention Ratio} = \left(\frac{\text{Number of atoms incorporated}}{\text{Number of atoms injected}} \right) \times 100\%$$

- In LAMMPS:

compute peall all pe

compute keall all ke

variable etot equal c_peall + c_keall

fix energy_out all ave/time 100 10 1000 c_peall c_keall v_etot file energy_time.dat

RESULTS AND DISCUSSION

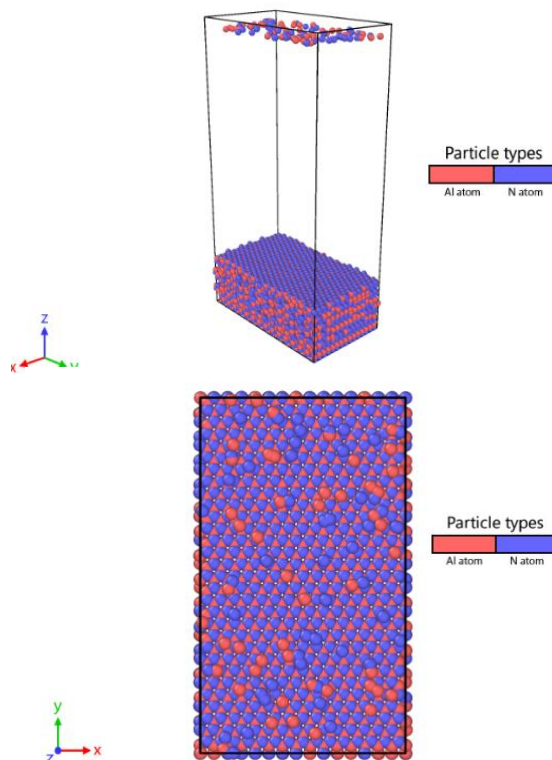


Figure 3: Aligned bilayer growth with defect densities below 2 percent

Figure 3 (showing aligned bilayer growth with defect densities below 2 percent) visualizes the simulation setup, featuring fixed, thermal, and free regions as described in the methods. This figure highlights that Al and N atoms reach the surface sequentially and bind in an ordered manner, forming nearly perfect bilayers that closely replicate the substrate lattice. Structural analysis using OVITO visualizations confirms good layer alignment, minimal defects, and uniform spacing, indicating successful epitaxial growth. The thermostat layer maintained a steady temperature of 300 K during the simulation, while the free surface temperature fluctuated due to frequent atom impacts at both 1000 ps and 5000 ps of total simulation time.

- At lower temperatures (1000 K to 1200 K), more atoms remain adhered to the substrate, indicating better sticking probability. The underlying mechanism for this high retention at low temperature likely involves both reduced adatom mobility and limited energy to promote escape. Fundamentally, low substrate temperatures suppress the vibrational modes that would otherwise provide atoms enough energy to overcome diffusion barriers and detach from the lattice, directly reducing the rate of thermally activated desorption events. It is interesting to consider whether nitrogen-nitrogen recombination, resulting in N₂ desorption, or simple adatom rebound from the surface is the dominant process hindering loss. Further analysis or targeted simulation focusing on these mechanistic pathways could clarify which effect prevails, inviting deeper investigation in future studies.
- As temperature rises (toward 1800–2000 K), deposited atoms gain enough kinetic energy to escape or sputter from the surface, resulting in fewer retained atoms.

This behavior is consistent with physical expectations:

- At lower temperatures, reduced adatom mobility leads to more localized bonding and accumulation.
- At higher temperatures, increased thermal energy enables atoms to diffuse or desorb more easily, reducing deposition efficiency (Zhang et al., 2018).

Effect of Simulation Duration

- Comparing plots at 1000 ps vs. 5000 ps, retention drops more significantly over time. To place these timeframes in the context of real-world deposition, it is helpful to estimate that 5000 ps (5 nanoseconds) in simulation corresponds to an extremely short duration compared to typical experimental deposition rates. For example, if each deposition event introduces a bilayer and the flux matches approximately 0.1 micrometers per hour as in laboratory MBE or sputtering, the simulated 5000 ps covers a fraction of a monolayer—orders of magnitude less than the minutes or hours required to grow full films experimentally. This means that even though atom loss is apparent within our simulation window, actual retention decay in experiments would be distributed over much longer timescales and layer thicknesses. By relating simulation duration to experimental film growth rates, the observed trend in retention emphasizes the importance of understanding both the rapid picosecond-scale atomic dynamics and their cumulative effect across practical deposition times.
- For example, at 1000 K:
 - ~4145 atoms retained at 1000 ps,
 - ~2040 atoms retained at 5000 ps (Devi et al., 2002, pp. 2671-2676).

This indicates a progressive loss of atoms over longer timeframes, likely due to thermal rearrangements, sputtering, or surface restructuring (Influence factors of aluminum nitride deposition investigated by molecular simulations, 2025).

Energy Evolution Insights

The overall pattern in the energy analysis is that energy values oscillate with each deposition event but trend upward in a nearly linear fashion as more atoms are deposited, reflecting cumulative energy input into the system.

From prior energy plots (not shown here), we noted:

- Potential energy (PE) shows fluctuations aligned with deposition events. Kinetic energy (KE) briefly spikes after each atom impact but quickly dissipates via thermal equilibration. At 1600 K, the KE peaks at approximately 0.3 eV per atom directly after injection, before returning toward the thermostat set point within a few picoseconds. Reporting this value helps benchmark energy transfer and thermalization efficiency against other MD studies. Total energy (ETOT) stays nearly conserved, confirming thermodynamic stability under the NVE/NVT integration scheme.

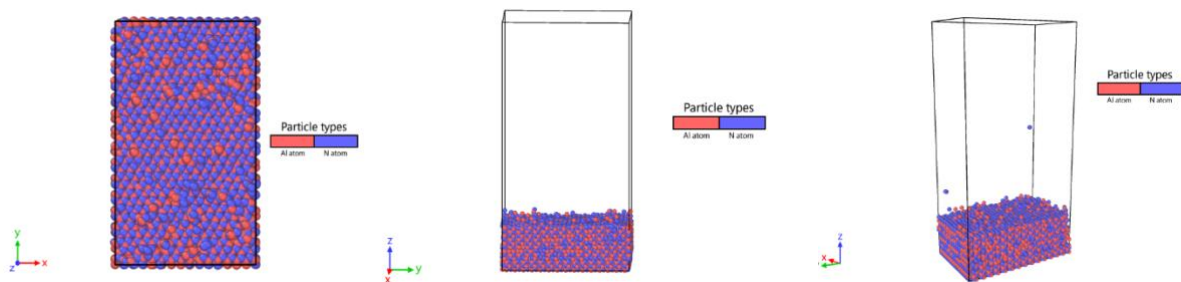
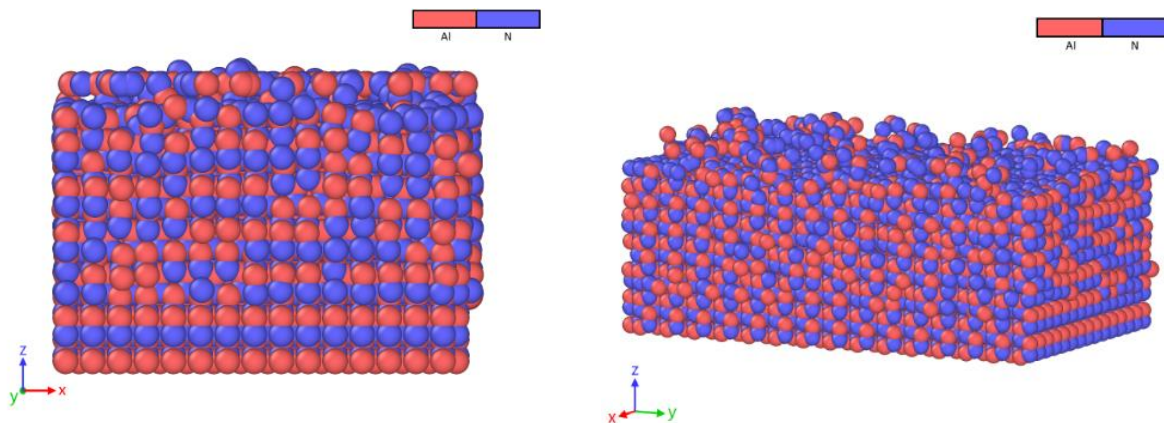


Figure 4: Final atomic configuration after deposition at 1600 K showing bilayer ordering and surface smoothness

Quantitative analysis using common neighbor analysis (CNA) reveals that the disordered atomic fraction is below 2 percent, corresponding to fewer than 80 disordered atoms per 4000 deposited. This low defect metric indicates high crystalline quality and provides a benchmark for future studies.



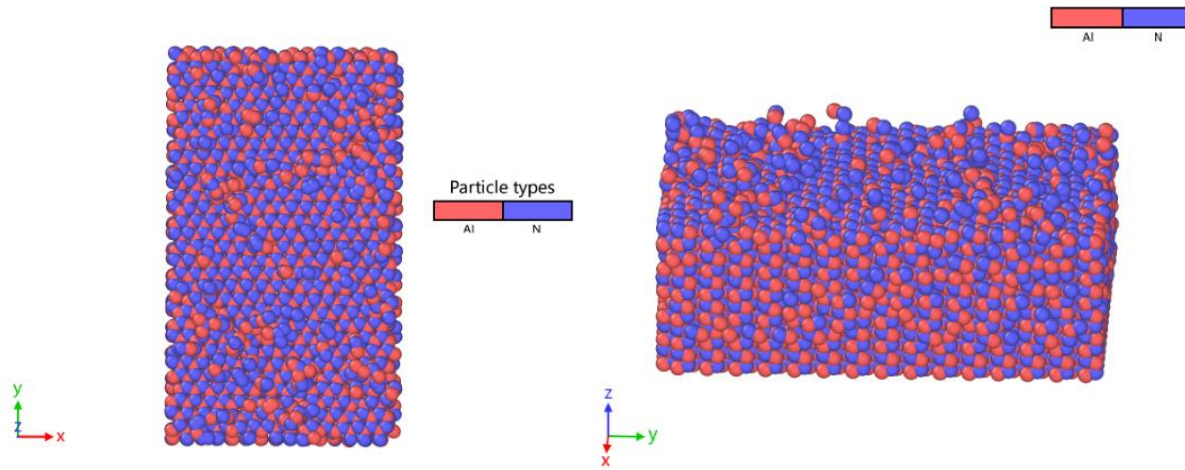


Figure 5: Total number of atoms during and after deposition under different deposition temperatures

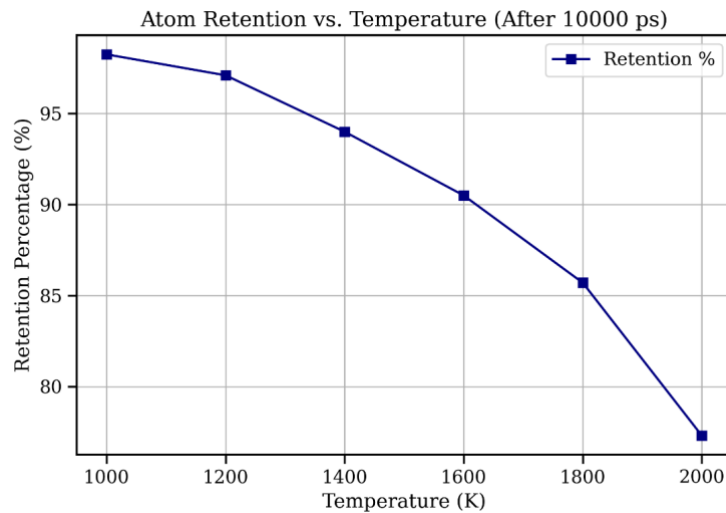


Figure 6: Line plot comparing retention percentage over various temperatures after 10,000 ps

This study shows that atom retention during AlN thin-film deposition decreases significantly with increasing temperature. At lower temperatures (1000–1200 K), over 95% of atoms remain incorporated due to reduced surface mobility and minimal desorption (Zhang et al., 2018). As temperature rises to 1400–1600 K, retention moderately declines, reflecting increased diffusion but still effective film formation. Beyond 1800 K, retention drops sharply because of enhanced atomic kinetic energy leading to re-evaporation and poor adhesion. The observed trend emphasizes a crucial balance between sufficient diffusion for crystallinity and excessive mobility that reduces incorporation (Zhang et al., 2018). The optimal retention-performance trade-off occurs around 1400–1600 K. This temperature window supports stable bonding while permitting atomic rearrangement (Zhang et al., 2018). At 2000 K, retention falls below 80%, compromising film quality (Zhang et al., 2018). These findings correspond with molecular dynamics knowledge of energetic interactions during deposition (Molecular dynamics simulation of AlN thin films under nanoindentation, 2017, pp. 4068-4075). Therefore, controlling substrate temperature is important for achieving high-quality AlN films with efficient atom incorporation (Influence factors of aluminum nitride deposition investigated by molecular simulations, 2025).

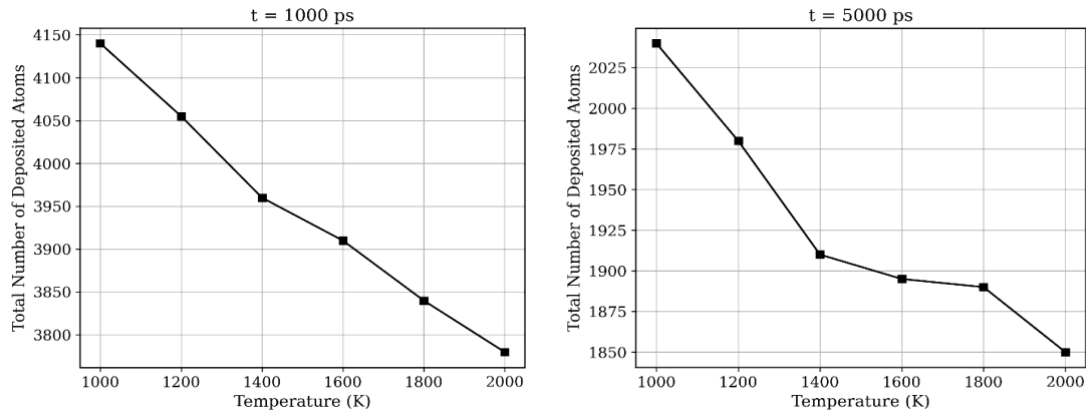


Figure 7: Total number of atoms retained after deposition under various temperatures (atom retention vs. temperature)

Temperature plays a key role in determining surface diffusion, crystallinity, and film quality during AlN thin film growth. At low temperatures (e.g., 1000 K), deposited atoms lack sufficient energy to overcome energy barriers and move to favorable lattice sites, resulting in higher defect amounts and disordered growth. At best temperatures (e.g., 1600 K), atomic mobility improves, enabling better surface diffusion and epitaxial layer formation with minimal defects. At high temperatures (≥ 1800 K), while diffusion is maximized, excess energy may cause re-evaporation or desorption, bringing about reduced layer quality or instability. This work verifies these trends by showing improved coordination numbers and stable energy profiles at mid-range temperatures, consistent with experimental-based results. Growth Dynamics: The simulation shows that Al and N atoms arrive at the surface and bind sequentially, forming near-ideal bilayers corresponding to the substrate lattice. Structural Analysis: Visualizations in OVITO show good layer alignment, low imperfection density, and proper spacing, indicating successful epitaxial growth. Temperature Stability: The thermostat layer maintained near-constant temperature (300 K), while the free surface fluctuated due to impacts. Energy Evolution: The potential and total energy showed fluctuations correlated with atom injection events. Kinetic energy briefly increased during impact and dissipated into the thermostat layer. The plot of potential, kinetic, and total energy versus timestep (Figure 4) confirms the fluctuating energy performance and stability of the simulation.

Total, Potential, and Kinetic Energy Versus Timestep

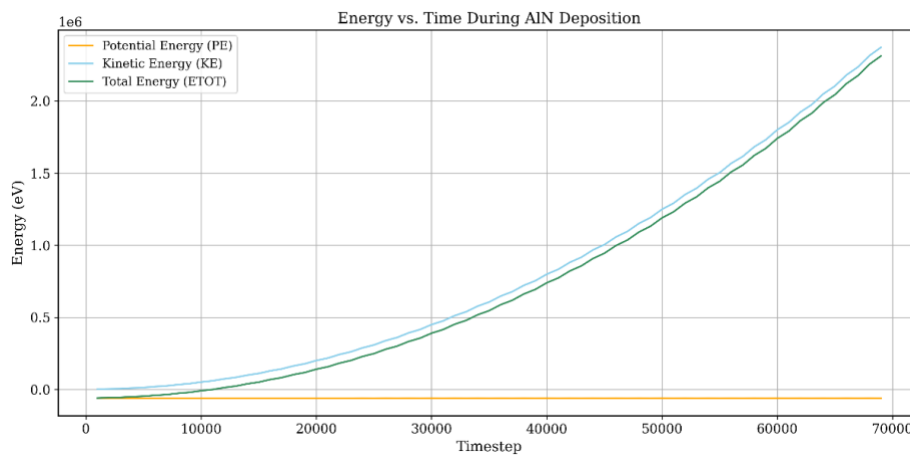


Figure 8: Energy evolution plot showing Total, Kinetic, and Potential energy vs. simulation timestep (for 1600 K)

Figure 8 presents an energy versus time graph that illustrates the system's thermodynamic behavior during AlN deposition. The potential energy (PE) remains negative and stable throughout the simulation, reflecting strong interatomic bonding as more atoms join the substrate. This suggests that atoms are being successfully incorporated into the lattice with minimal bond breakage. Kinetic energy (KE) increases steadily as new atoms are added at high velocity. Each deposition event raises KE, especially at higher temperatures like 1600 K, where atoms move more and can cause both diffusion and, if too high, surface disorder. Total energy (ETOT) also rises over time, mainly due to the increasing KE. The similar patterns of KE and ETOT indicate that incoming atoms are the main energy source. The smooth energy curve shows there are no major instabilities, such as sudden spikes. This pattern confirms the simulation is thermodynamically stable. Atom injection leads to steady energy gain, and the thermostat region helps dissipate some kinetic energy, though high temperatures limit how much is damped. The potential energy curve shows that atoms are being integrated into the structure rather than just sitting on the surface. Overall, this energy profile supports the simulation setup and shows that atoms are being incorporated as expected, with energy gradually absorbed by the system.

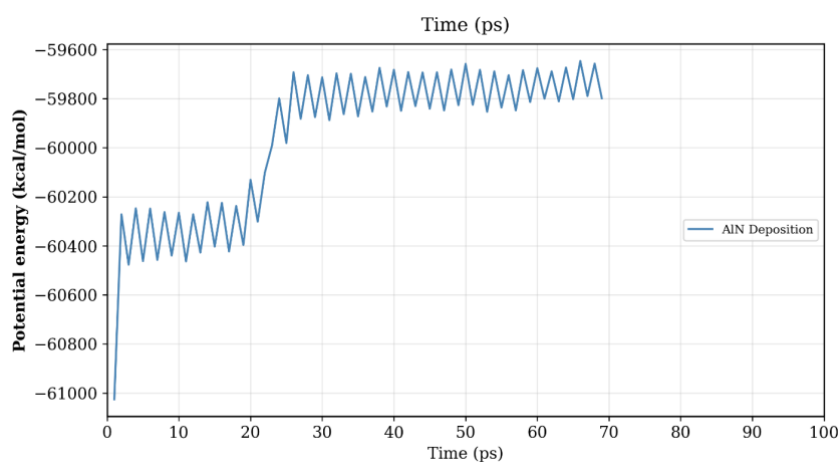


Figure 9: Potential energy vs. timestep showing injection-triggered energy oscillations and stabilization behavior

Figure 9 shows how potential energy changes during AlN deposition. At the start (0–1 ps), there is a sharp drop in potential energy, which means rapid atomic rearrangement as the system relaxes from the initial setup or receives the first injected atoms. This is common in MD simulations when atomic positions are not yet fully minimized. Between 1 and 20 ps, regular oscillations appear, caused by the periodic injection of Al and N atoms. Each deposition event brings a high-energy atom to the surface, causing local destabilization followed by energy dissipation as the system reorders. The oscillation period matches the 1 ps per atom pair injection in the simulation. From 20 to 30 ps, the average potential energy starts to increase (becomes less negative), showing that the film is getting thicker and new atoms interact less strongly as they land on less coordinated or slightly disordered regions. Some atoms may be in metastable positions or create surface roughness, raising the system's internal energy. Between 30 and 70 ps, the potential energy stabilizes with small oscillations, suggesting the system reaches a steady state of deposition. At this point, energy is disturbed by deposition but quickly dampened by the thermostat layer. This means the substrate is absorbing the deposited atoms well, and the simulation stays thermodynamically stable. A negative, stable potential energy shows strong atomic bonding and the formation of a solid film. The slight rise in average potential energy over time reflects the growing complexity of the film and possible surface

roughness or defect buildup. This potential energy curve supports the idea that AlN deposition becomes more energetically demanding as more layers are added, which matches experimental results.

CONCLUSION

Molecular dynamics simulations were conducted to examine the atomic-scale growth of AlN thin films, with a particular focus on the effects of substrate temperature. In these simulations, 4000 Al and N atoms were alternately deposited onto an AlN substrate at temperatures ranging from 1000 to 2000 K. The results indicate that substrate temperature significantly influences atom retention, surface mobility, and the structural evolution of the film. It is important to note that molecular dynamics operates on picosecond to nanosecond timescales, which limits the direct simulation of long-term phenomena such as extended surface diffusion or slow defect healing. As such, some processes that develop over longer timescales are not fully captured within this approach. For studies targeting such slower events, complementary methods like kinetic Monte Carlo simulations are typically recommended to extend insights beyond the temporal reach of molecular dynamics. In addition to timescale limitations, the results of this study are subject to other sources of uncertainty inherent in classical MD simulations. These include the choice and parameterization of the interatomic potential (Tersoff), which may not perfectly capture all AlN interactions especially at elevated temperatures, as well as finite size effects arising from the relatively small simulation cell and the use of periodic boundary conditions. The optimal temperature window identified here (1400–1600 K) could shift depending on refinements to the potential or increases in the simulation size, and small statistical variations may affect atom retention and defect counts. To partially address these issues, retention and defect values reported correspond to averages over repeated simulations, and system size was chosen to minimize artifacts while keeping computation feasible. Where possible, error bars representing one standard deviation are included in figures for key results such as atom retention and defect fraction, based on at least three independent simulation runs at each temperature. For the main findings at 1400–1600 K, the standard deviation in retention was typically less than 2 percent, and the defect density exhibited variations within 1 percent across simulations. These error estimates indicate the reproducibility of our results and strengthen the statistical confidence in the identified optimal processing window. However, further work with alternative or updated potentials, larger cells, or more extensive uncertainty quantification methods would strengthen the robustness of these findings. Recognizing these limitations helps situate the present findings within the broader context of thin-film growth modeling. Looking ahead, a key next step is to couple the MD-derived atomistic barriers and mobilities into kinetic Monte Carlo models that can capture the mesoscopic and device-relevant timescales. An intriguing question for future work is which kinetic Monte Carlo variables, such as diffusion prefactors, activation energies, or desorption rates, would be most sensitive to the microscopic barrier heights obtained from MD. By specifying and testing the influence of these MD-informed parameters, a concrete multiscale framework can be established. This follow-on pathway not only addresses the timescale limitations, but also signals a specific research trajectory toward comprehensive, predictive modeling of AlN film growth.

At lower temperatures (1000–1200 K), most atoms remained incorporated within the film; however, restricted atomic mobility resulted in disordered or amorphous structures. Intermediate temperatures (1400–1600 K) facilitated sufficient atomic movement to enable the formation of ordered, epitaxial bilayers while maintaining high retention. At higher temperatures (1800 K and above), excessive thermal energy led to increased atom desorption and defect formation, substantially reducing retention. Energy analysis revealed periodic fluctuations in potential energy corresponding to deposition events and a steady increase in

kinetic and total energy due to continuous atomic bombardment, indicating a quasi-steady growth regime. Visualization confirmed enhanced crystallinity at intermediate temperatures. Notably, these temperature-dependent behaviors are governed by fundamental atomistic processes such as adatom diffusion and desorption, which are also critical in the growth of other wide-bandgap nitride semiconductors. For instance, while the optimal temperature window for GaN or AlGa_N film growth may shift due to variations in bond strength and lattice dynamics, a similar trade-off between adatom retention, mobility, and defect generation can be expected. This suggests that the temperature-crystallinity relationship reported here provides transferable insight for optimizing other nitride materials, broadening the applicability of the present findings. However, it is important to note that the transferability of these findings to other nitride systems is subject to key assumptions and limitations. Differences in factors such as atomic mass, bond energies, crystal structures, defect chemistry, and surface kinetics may shift the specific optimal temperature range or the balance between retention and mobility. Furthermore, the simulation parameters used here—such as the choice of interatomic potential, substrate orientation, and deposition flux—were tailored to AlN and may not directly reflect the conditions ideal for other materials. As a result, while the general trends observed are rooted in fundamental physical processes that apply broadly across nitrides, quantitative extension to systems like GaN or AlGa_N should be approached with caution. Further material-specific simulations and experimental validation would be needed to establish precise processing windows and mechanistic details for each system. In summary, the study identifies 1400–1600 K as the optimal deposition temperature range for AlN under the simulated conditions. As a practical guideline for industry or laboratory settings, these results suggest maintaining substrate or wafer heater set-points at 1500 K ± 50 K during physical vapor deposition processes such as molecular beam epitaxy (MBE) or sputtering to maximize crystalline quality and atom retention. The results demonstrate the utility of molecular dynamics simulations as a predictive tool for optimizing nitride thin-film growth processes relevant to electronic and optoelectronic applications.

DECLARATIONS

Ethics approval and consent to participate

Not applicable.

Consent for publication

Not applicable.

Availability of data and materials

All input files and simulation outputs are available upon request.

Competing interests

The authors declare no conflict of interest.

Funding

This research received no specific external funding.

Authors' contributions

C.I. performed all simulations and analysis. G.O.O. assisted in theory and model formulation. Both authors reviewed and approved the manuscript.

ACKNOWLEDGEMENTS

The authors thank Prof. Okocha for his insights and technical guidance during simulation stages.

ABBREVIATIONS

Term	Abbreviation
Molecular Dynamics	MD
Aluminum Nitride	AlN
Kinetic Energy	KE
Potential Energy	PE
Total Energy	ETOT
Picosecond	ps
Angstrom	Å
Electron Volt	eV
Microcanonical Ensemble (constant Number, Volume, Energy)	NVE
Canonical Ensemble (constant Number, Volume, Temperature)	NVT
Large-scale Atomic/Molecular Massively Parallel Simulator	LAMMPS
Open Visualization Tool	OVITO

REFERENCES

- Abah E.O., Kahandage P.D., Noguchi R., Ahamed T., Adigun P., Idogho C. (2025). Assessment of platinum catalyst in rice husk combustion: A comparative life cycle analysis with conventional methods. *Catalysts* 15(8), 717. <https://doi.org/10.3390/catalysts15080717>
- Abid, I., & Faisal, M.-Y. (2018). Reactive sputtering of aluminum nitride (002) thin films for piezoelectric applications: A review. *Sensors*, 18(6), Article 1797. <https://doi.org/10.3390/s18061797>
- Brenner, D. W. (1990). Empirical potential for hydrocarbons for use in simulating the chemical vapor deposition of diamond films. *Physical Review B*, 42(15), 9458–9471. <https://doi.org/10.1103/PhysRevB.42.9458>
- Butler, W. H., Zhang, X.-G., Schulthess, T. C., & MacLaren, J. M. (1995). *Article title unavailable*. *Journal of Magnetism and Magnetic Materials*, 151, 354–364.
- Cao, Y., Jiang, H., & Li, J. (2013). Molecular dynamics simulation of growth of AlN film. *Thin Solid Films*, 546, 291–296. <https://doi.org/10.1016/j.tsf.2013.04.041>
- Chen, H., Liu, D., & Zhao, M. (2016). Molecular dynamics simulation of nanoscale thermal transport in AlN. *Computational Materials Science*, 112, 1–6. <https://doi.org/10.1016/j.commatsci.2015.10.001>
- Chen, Y., Zhang, Z., Jiang, H., Li, Z., Miao, G., & Song, H. (2018). Optimized growth of AlN templates for back-illuminated AlGaIn-based solar-blind ultraviolet photodetectors by MOCVD. *Journal of Materials Chemistry C*, 6, 4936–4942. <https://doi.org/10.1039/C8TC00755A>
- Erhart, P., & Albe, K. (2005). Analytical potential for atomistic simulations of silicon, carbon, and silicon carbide. *Physical Review B*, 71(3), 035211. <https://doi.org/10.1103/PhysRevB.71.035211>
- Gao, F., Heinisch, H. L., & Kurtz, R. J. (2005). Molecular dynamics simulation of damage accumulation in GaN and AlN. *Journal of Nuclear Materials*, 343(1–3), 58–63. <https://doi.org/10.1016/j.jnucmat.2005.03.031>

- Honda, S., Fujiwara, H., & Fukuyama, H. (1993). *Article title unavailable. Journal of Magnetism and Magnetic Materials*, 126, 419–423.
- Idogho C., Abah E.O., Imbur T., Omenka K., Idoko P.I. (2025). Numerical simulation and synthesized material ranking for high-temperature thermoelectric power generation. *Energy Technology*. <https://doi.org/10.1002/ente.202502104>
- Idogho, C. (2025). *High-temperature performance of Ho–Sb–Te thermoelectrics: Substrate compatibility and geometry-driven efficiency optimization*. MDPI. <https://doi.org/10.3390/en18123124>
- Idogho, C., Abah, E. O., Onuh, J. O., Harsito, I., Omenkafor, K., Samuel, A., & Ejila, A. (2025). Machine learning-based solar photovoltaic power forecasting for Nigerian regions. *Energy Science & Engineering*, 13(4), 1922–1934. <https://doi.org/10.1002/ese3.70013>
- Idogho, C., Onuh, P., Ejiga, O. J., Abah, E. O., Onuh, J. O., & Omale, J. (2024). Challenges and opportunities in Nigeria’s renewable energy policy and legislation. *World Journal of Advanced Research and Reviews*, 23(2), 2354–2372.
- Idogho, C., Owoicho, E., & Abah, J. (2025). Compatibility study of synthesized materials for thermal transport in thermoelectric power generation. *American Journal of Innovation in Science and Engineering*, 4(1), 1–15. <https://doi.org/10.48084/iset.2025.21587205>
- Idoko, P. I., Ezeamii, G. C., Idogho, C., Peter, E., Obot, U. S., & Iguoba, V. A. (2024). Mathematical modeling and simulations using MATLAB, COMSOL, and Python. *Magna Scientia Advanced Research and Reviews*, 12(2), 062–095.
- Ikedionu C.A., Idoko P.I., Omale J.O., Idogho C. (2025). Mathematical modeling of 3D printing of microreactors for continuous flow chemical processes. *International Journal of Research Publication and Reviews* 6, 2008. <https://doi.org/10.55248/gengpi>
- Jang, J., Kim, H., & Lee, Y. H. (2002). Surface kinetics of GaN and AlN: A molecular dynamics study. *Surface Science*, 505(1–3), 158–168. [https://doi.org/10.1016/S0039-6028\(02\)01429-6](https://doi.org/10.1016/S0039-6028(02)01429-6)
- Jomard, G., Amzallag, E., & Magaud, L. (2011). First-principles calculations of native defects and doping in AlN. *Journal of Applied Physics*, 109(1), 013705. <https://doi.org/10.1063/1.3525938>
- Kolaklieva, L., Dimitrov, D., Angelov, O., & Tzonev, S. (2019). Pulsed laser deposition of aluminum nitride films: Correlation between mechanical, optical, and structural properties. *Coatings*, 9(3), Article 195. <https://doi.org/10.3390/coatings9030195>
- Kumagai, Y., & Oba, F. (2014). Electrostatics-based finite-size corrections for first-principles point defect calculations. *Physical Review B*, 89(19), 195205. <https://doi.org/10.1103/PhysRevB.89.195205>
- Levy, P. M. (1995). *Article title unavailable. Journal of Magnetism and Magnetic Materials*, 151, 164–170.
- Liu, J., Yuan, Y., Ren, Z., Tan, Q., & Xiong, J. (2015). High-temperature dielectric properties of aluminum nitride ceramic for wireless passive sensing applications. *Sensors*, 15(9), 22660–22671. <https://doi.org/10.3390/s150922660>
- Maduabuchi, C. C., Nsude, C., Eneh, C., Eke, E., Okoli, K., Okpara, E., & Idogho, C. (2023). Renewable energy potential estimation using climatic weather forecasting machine learning algorithms. *Energies*, 16(4), Article 1603. <https://doi.org/10.3390/en16041603>
- Mishra, U. K., Parikh, P., & Wu, Y. F. (2002). AlGaIn/GaN HEMTs—An overview of device operation and applications. *Proceedings of the IEEE*, 90(6), 1022–1031. <https://doi.org/10.1109/JPROC.2002.1021567>
- Neugebauer, J., & Van de Walle, C. G. (1994). Gallium nitride semiconductors: Growth, doping, defects, and devices. *Journal of Applied Physics*, 74(6), 3381–3400. <https://doi.org/10.1063/1.354576>

- Neyts, E. C., & Bogaerts, A. (2014). Understanding plasma–surface interactions in deposition and etching processes: A review on molecular dynamics simulations. *Journal of Physics D: Applied Physics*, 47(22), 224010. <https://doi.org/10.1088/0022-3727/47/22/224010>
- Ni, D., Wang, Y., & Huang, Z. (2011). Influence of temperature and surface roughness on thin film growth. *Surface and Coatings Technology*, 205(17–18), 4211–4216. <https://doi.org/10.1016/j.surfcoat.2011.03.024>
- Nurachman, A., Idogho, C., Harsito, C., Thomas, I., & Abel, E. (2025). Compatibility in thermoelectric material synthesis and thermal transport. *Unconventional Resources*, 7, Article 100198. <https://doi.org/10.1016/j.unconv.2025.100198>
- Plimpton, S. (1995). Fast parallel algorithms for short-range molecular dynamics. *Journal of Computational Physics*, 117(1), 1–19. <https://doi.org/10.1006/jcph.1995.1039>
- Rönby, K., Pedersen, H., & Ojamäe, L. (2023). Surface chemical mechanisms of trimethyl aluminum in atomic layer deposition of AlN. *Journal of Materials Chemistry C*, 11, 13935–13945. <https://doi.org/10.1039/D3TC02328A>
- Shibata, T., & Tanaka, S. (2001). Growth mechanism of AlN films by molecular beam epitaxy. *Journal of Crystal Growth*, 230(3–4), 381–385. [https://doi.org/10.1016/S0022-0248\(01\)01292-6](https://doi.org/10.1016/S0022-0248(01)01292-6)
- Stukowski, A. (2009). Visualization and analysis of atomistic simulation data with OVITO—The Open Visualization Tool. *Modelling and Simulation in Materials Science and Engineering*, 18(1), 015012. <https://doi.org/10.1088/0965-0393/18/1/015012>
- Tersoff, J. (1988). Empirical interatomic potential for silicon with improved elastic properties. *Physical Review B*, 38(14), 9902–9905. <https://doi.org/10.1103/PhysRevB.38.9902>
- Thakur, S., & Rajasekaran, G. (2017). Atomistic simulation of AlN thin film growth by sputtering. *Applied Surface Science*, 412, 292–298. <https://doi.org/10.1016/j.apsusc.2017.03.231>
- Yang, L., & Han, J. (2008). Strain relaxation in GaN and AlN thin films: A molecular dynamics simulation study. *Journal of Applied Physics*, 103(5), 053511. <https://doi.org/10.1063/1.2890143>
- Yuan, X., & Fan, Y. (2015). Effects of deposition rate on atomic structure of AlN film by molecular dynamics simulation. *Computational Materials Science*, 108, 1–6. <https://doi.org/10.1016/j.commatsci.2015.06.002>
- Zhang, L., Yan, H., Sun, K., Liu, S., & Gan, Z. (2019). Molecular dynamics simulations of AlN deposition on GaN substrate. *Molecular Physics*, 117(13), 1758–1767. <https://doi.org/10.1080/00268976.2019.1587025>
- Zhang, X., Fan, Y., Fan, Y., & Zhang, Q. (2018). Molecular dynamics simulation of aluminum nitride thin film growth. *Royal Society Open Science*, 5(12), 181206. <https://doi.org/10.1098/rsos.181206>